

Vibrational spectroscopic study of ferroelectric SbNbO_4 , antiferroelectric BiNbO_4 , and their solid solutions

Pushan Ayyub, M. S. Multani, V. R. Palkar, and R. Vijayaraghavan
Tata Institute of Fundamental Research, Homi Bhabha Road, Bombay 400005, India
 (Received 23 May 1986)

Raman scattering and infrared absorption studies of ferroelectric SbNbO_4 , antiferroelectric BiNbO_4 , and the solid solution $(\text{Sb}_{1-x}\text{Bi}_x)\text{NbO}_4$ for $0 < x < 1$ in the range 20–1200 cm^{-1} are reported. These are the first vibrational spectroscopic investigations in these stibiotantalite-type systems. Symmetry assignments are proposed for the internal modes. Such an assignment is shown to lead to a consistent set of values for the local force constants calculated under the general quadratic valence force field. The nature of the variations of lattice and internal frequencies with changes in A^{3+} -ion concentration is qualitatively discussed with particular reference to the ferroelectric soft mode.

I. INTRODUCTION

The ABO_4 family of compounds possessing stibiotantalite structure (with $A = \text{Bi}^{3+}, \text{Sb}^{3+}$, and $B = \text{Nb}^{5+}, \text{Ta}^{5+}, \text{Sb}^{5+}$) have generated considerable interest in recent years. These compounds are known to exhibit multiple structural and dielectric phase transitions, but the exact nature of these transitions, as well as the mechanism of ferroelectricity, is not completely understood. In addition, some of them possess excellent ferroelectric and piezoelectric properties and are important potential candidates for device fabrication. The syntheses, structural, and dielectric properties of ABO_4 single crystals have been reviewed by Popolitov, Lobachev, and Peskin.¹ The only vibrational investigation in these compounds known to the authors is an ir absorption study² of $\text{Sb}(\text{Sb}_x\text{Nb}_{1-x})\text{O}_4$. In this paper we report for the first time Raman scattering and ir absorption results on SbNbO_4 , BiNbO_4 , and the solid-solution system $(\text{Sb}_{1-x}\text{Bi}_x)\text{NbO}_4$. The syntheses of these polycrystalline materials and their structural and dielectric data will be reported separately.³

BiNbO_4 is antiferroelectric (AFE) at room temperature (RT) but becomes ferroelectric (FE) at 360°C and paraelectric at 570°C. Conversely, SbNbO_4 is FE at RT, AFE above 410°C, and paraelectric above 605°C. The orthorhombic unit cells in the ABO_4 compounds contain four formula units. Typically, the stibiotantalite structure consists of layers of vertex-sharing, distorted BO_6 octahedra parallel to the (001) plane. It has been suggested¹ that the off-center displacements of the Sb^{3+} ions in highly distorted oxygen-polyhedral environments may lead to the spontaneous polarization in SbNbO_4 . The A sublattice is believed to be ferroelectrically active for the following reasons: (a) the transition temperatures in the ABO_4 series depend mainly on the nature of A and are practically independent of B ; (b) on replacing B by a pair of cations of different valences such that overall electro-neutrality and stoichiometry are maintained (e.g., $\text{SbMg}_{0.25}^2\text{W}_{0.75}^6\text{O}_4$), the T_C is found to be only weakly dependent on the ionic radii, valences, and polarizabilities of the B -site substituents;⁴ and (c) relatively large "rattle space" is available to the Sb^{3+} ions, since the unit-cell di-

mensions are quite comparable in SbNbO_4 and BiNbO_4 , but the ionic radius of Sb^{3+} is almost 25% smaller than that of Bi^{3+} .

II. EXPERIMENTAL

Raman spectra were recorded from powder samples either in capillary tubes or as pellets using a SPEX model No. 1403 double monochromator. The exciting radiation was the 514.5-nm green line from a Spectra Physics Ar^+ laser operated nominally at 200 mW. A third monochromator was used to investigate low-energy modes. The spectra were scanned at a rate of 1 $\text{cm}^{-1}\text{s}^{-1}$ with a 1 cm^{-1} resolution and summed over 3–4 scans. The wave-number accuracy was estimated at 1.5 cm^{-1} and the precision at 1 cm^{-1} . Plasma lines were eliminated from the incident radiation by a grating element. The dispersed light was detected by a thermoelectrically cooled photomultiplier. Infrared absorption spectra were recorded on a Nicolet model No. 170SX FT-IR instrument with the samples in the form of pellets (dispersed in KBr) for the 400–1200 cm^{-1} region.

The RT phase of SbNbO_4 belongs to the $Pna2_1$ (C_{2v}^9) space group in which the only allowed site symmetry is C_1 . The 24-atom unit cell allows for 72 normal vibrations. Using nuclear site group analysis,⁵ we may classify the optic phonons into the following irreducible representations:

$$\Gamma = 17A_1 + 18A_2 + 17B_1 + 17B_2 .$$

All the modes are Raman active and all except the A_2 modes are ir active as well. On the other hand, BiNbO_4 has the $Pnna$ (D_{2h}^6) structure at RT. Since it is believed⁶ to be isostructural to α - SnWO_4 , we expect the four Bi^{3+} ions to occupy C_2^2 sites and the four Nb^{5+} ions to occupy C_2^2 sites. Two distinct sets of eight O^{2-} ions are all in general (C_1) positions. The optic phonons can be classified as

$$\Gamma = 8A_g + 8A_u + 9B_{1g} + 8B_{1u} + 10B_{2g} + 9B_{2u} + 9B_{3g} + 8B_{3u} .$$

Of these, all *gerade* modes are Raman active and all *ungerade* modes except A_u are ir active. The mutual ex-

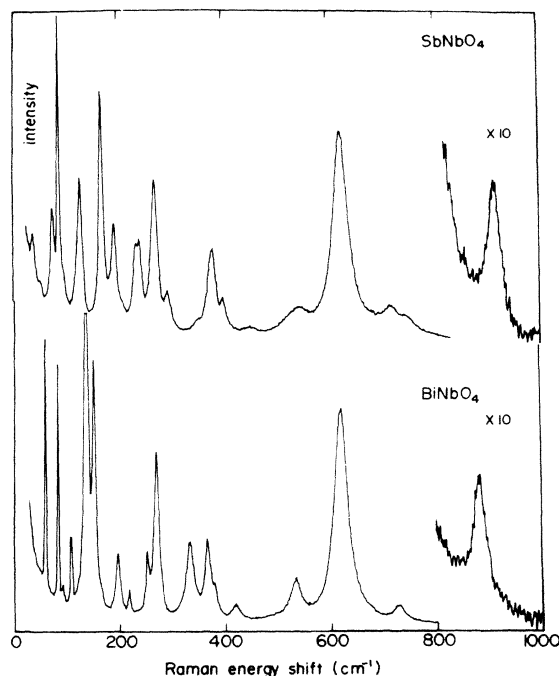


FIG. 1. Room-temperature Raman spectra of SbNbO_4 and BiNbO_4 .

TABLE I. Vibrational spectra of SbNbO_4 and BiNbO_4 and assignment of observed lines to the symmetry species of NbO_6 octahedra. (s=strong, m=medium, w=weak, b=broad, sh=shoulder, db=doublet, v=very). Unit: cm^{-1} .

SbNbO_4		BiNbO_4		Symmetry assignment
Raman	Infrared	Raman	Infrared	
37w-m	25m		28w-m	
54vw	53s	60s	35w-m	
75s		84s	83m	
87vs	89w,sh	93w		
	122m	108	120m	
128s	131m	110 ^{m,db}		
	141m	139vs	130m	
168vs	151vs	153vs	156vs	
	182s,b		165,174db	
192s		199m	198m	$F_{2u}(\nu_6)$
232	210s	220w-m	208m	
239 ^{m,db}	228m	255m	232s	
269s		272s		$F_{2g}(\nu_5)$
292w	290w		289s	
	303m	336m-s	328w,sh	
	327m		347sh	
	352vs		356vs	$F_{1u}(\nu_4)$
377m-s	380m	368m-s	374w,sh	
397w-m	397,419sh	382w		
448w	462s,b	424w	422m	
	476m		433m	
	486m		442m	
542w-m		537w-m		$E_g(\nu_2)$
	600vs,vb		580vs,vb	$F_{1u}(\nu_3)$
620vs,b		624vs,b		$A_{1g}(\nu_1)$
718w,b	692w		642s,b	
740vw	720w	730w	716s,b	
913w	910w	883w		

clusion of the Raman and ir modes is caused by the inversion symmetry of the lattice. In practice it would be impossible to observe all the predicted modes in polycrystalline samples due to the low polarizabilities of some of these modes as well as the overlap of incompletely resolved modes. Even though all frequencies cannot be identified unequivocally in the absence of single-crystal data, one can nevertheless obtain significant information regarding the dynamics of the basic structural units and the soft modes from studies of the polycrystalline material. RT Raman spectra of SbNbO_4 and BiNbO_4 are shown in Fig. 1. The frequencies of all Raman and ir lines observed in these materials are collected in Table I.

III. MODE ASSIGNMENTS AND FORCE-CONSTANT CALCULATIONS

In metal oxide systems involving Nb^{5+} , the intragroup binding energy within the NbO_6 octahedra is large compared to the intergroup or crystal binding energy.⁷ In addition, these octahedra are not greatly distorted from the ideal O_h symmetry in either of the two oxides being studied. This allows us to adopt the "internal mode" approach, where, as a first approximation, we may interpret the vibrational spectra as arising from the internal vibrations of (perfect) NbO_6 octahedra plus the external vibrations. The latter occur at much lower frequencies and arise from cation-octahedral and intergroup oscillations. The vibrational modes of a perfect, isolated BO_6 octahedron and the correlations that they bear with the vibrations allowed by D_{2h} symmetry (as in BiNbO_4), are indicated in Fig. 2. Of the BO_6 (O_h) modes two are pure bond-stretching vibrations ($A_{1g} + E_g$), two are interbond angle-bending vibrations ($F_{2g} + F_{2u}$), and the remaining (F_{1u}) is a combination of both. The g modes are only Raman active, and the F_{1u} mode only ir active. The F_{2u} mode is silent in O_h but observable when the local symmetry is lowered.

The ν_1 (A_{1g}) Raman mode arises from the symmetric

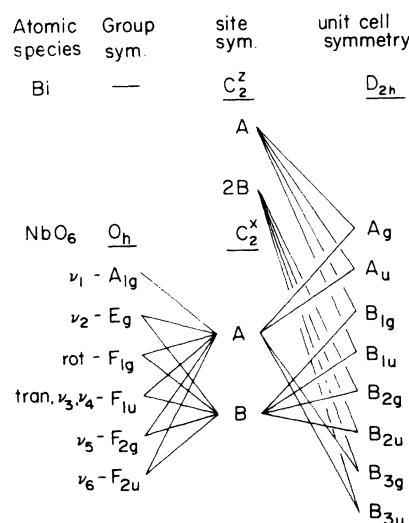


FIG. 2. Correlation table for the BiNbO_4 vibrational spectra. The frequencies of the perfect NbO_6 octahedron are related to those occurring in the actual unit-cell symmetry (D_{2h}).

Nb-O stretching vibration and is normally the strongest among the higher-frequency modes. In the present case the strong, broad Raman band around 620 cm^{-1} is almost certainly the ν_1 mode. The ν_2 (E_g) mode occurs at a somewhat lower frequency and is considerably weaker in such systems; so this symmetry is assigned to the line near 540 cm^{-1} . The ν_5 (F_{2g}) Raman mode is expected to be intense and may be identified with the strongest line in the $250\text{--}310\text{ cm}^{-1}$ region, i.e., the one around 270 cm^{-1} . The F_{1u} stretching (ν_3) and bending (ν_4) modes appear strongly in the ir spectra in the 600 cm^{-1} and 350 cm^{-1} regions, respectively. The low-frequency line appearing in both Raman and ir spectra in the $190\text{--}200\text{ cm}^{-1}$ region is expected to belong to the ν_6 (F_{2u}) symmetry. The symmetry assignments for the observed frequencies are displayed in Table I. It is reasonable to expect the rather weak lines around $880\text{--}910\text{ cm}^{-1}$ and $720\text{--}730\text{ cm}^{-1}$ to arise from stretching vibrations of the A^{3+} ions in their highly distorted oxygen-octahedral surroundings. Such an argument is supported by the rapid decrease with x shown by the line near 900 cm^{-1} in the $(\text{Sb}_{1-x}\text{Bi}_x)\text{NbO}_4$ system (note that the mass of A^{3+} effectively increases with x). Other unassigned lines (mainly in the $220\text{--}450$ region)

can be interpreted in terms of correlation-field splittings of the ideal NbO_6 modes in the lower site symmetry of the lattice.

The local force constants were calculated under the general quadratic valence-force-field approximation.⁸ The force-constant matrix elements (F_{ij}) for the BO_6 octahedron are expressed in terms of the local primary (f_p) and interaction (f_{pq}) force constants are shown in Table II. The latter are calculated from the observed vibrational frequencies using the FG matrix method⁹ which essentially consists of solving the secular determinant $|FG - E\lambda| = 0$, with the eigenvalues $\lambda = (2\pi\nu c)^2$. The G -matrix elements are functions of the $B\text{--}O$ bond distance ($r = \rho^{-1}$) and the inverse atomic masses μ_B and μ_O . Normally, the bending force constants occur only in combinations because all the angular deformation coordinates are not independent. This situation can be simplified by neglecting interactions between angles not having a common side, and between angles and bonds that do not form that angle. The interatomic force constants so calculated (Table II) are quite comparable to and follow the same trends as those determined by Ross¹⁰ for some other niobates, using a similar approach. Such agreement lends additional support to our assignment of vibrational modes.

TABLE II. Definitions of F matrix elements and interatomic force constants for BO_6 octahedra. Calculated values are in mdyn/\AA .

Force constants	Defining expressions	Calculated values for	
		SbNbO_4	BiNbO_4
F_{11}	$f_r + f'_{rr} + 4f_{rr}$	3.624	3.670
F_{22}	$f_r + f'_{rr} - 2f_{rr}$	2.769	2.718
F_{33}	$f_r - f'_{rr}$	2.912	2.877
F_{34}	$2(f'_{ra} - f_{ra})$	-0.378	-0.285
F_{44}	$(f_a - f''_{aa}) + 2(f_{aa} - f'''_{aa})$	1.388	1.324
F_{55}	$2(f_a - f''_{aa}) - (f_a - f'''_{aa})$	0.682	0.697
F_{66}	$(f_a - f''_{aa}) - 2(f_{aa} - f'''_{aa})$	0.695	0.747
f_r	$\text{BO bond stretching}$	2.983	2.956
f_{rr}	Interaction between bond stretches at 90°	0.142	0.159
f'_{rr}	Interaction between bond stretches at 180°	0.071	0.079
f_a	$\text{OBO angle deformation}$	1.042	1.035
f_{ra}	Interaction between BO stretch and OBO bend, with OBO including BO	0.189	0.143
f_{aa}	Interaction between angles with common side, other sides being at 90°	0.173	0.144
f'_{aa}	Interaction between angles with common side, other sides being at 180°	0.180	0.169

Note: (a) The remaining interactions ($f''_{aa}, f'''_{aa}, f'_{ra}$) are neglected. (b) It was assumed (following Ref. 10) that $f'_{rr} = f_{rr}/2$. (c) The F_{ij} are dimensionally adjusted (depending on the corresponding G_{ij}) so that $FG \sim \lambda$ has dimensions of s^{-2} .

IV. RAMAN SPECTRA OF $(\text{Sb}_{1-x}\text{Bi}_x)\text{NbO}_4$

The compounds SbNbO_4 and BiNbO_4 were found to form true solid solutions over the entire range of concentrations ($0 < x < 1$) with all the compositions belonging to the orthorhombic class. Powder x-ray diffraction data³ indicate the existence of three distinct regions (at RT) in the $x\text{--}T$ phase diagram, which may be denoted as I (based on the SbNbO_4 structure for $0 < x < 0.2$), II (intermediate region for $0.2 < x < 0.8$) and III (based on the BiNbO_4 structure for $0.8 < x < 1.0$). Raman spectra were recorded from samples with $x = 0.02, 0.1, 0.2, 0.3, \dots, 0.9$. The dependence of the Raman frequencies on x for the different modes is plotted in Fig. 3. For quite a few of these modes the $\nu\text{--}x$ curves show discontinuities near $x = 0.2$ and 0.8 , corroborating the phase demarcations mentioned above. Within any one phase, however, the dependence of ν on x is approximately linear.

The following additional observations may be made regarding the general features of the spectra. (a) Most of the Raman lines in these mixed systems are not appreciably broadened as compared to the pure end members. Such broadening would have indicated strong disorder effects due to the absence of long-range translational symmetry. (b) A weak mode at 990 cm^{-1} occurs exclusively in some of the solid solutions. This mode may be identified as a local (impurity) mode since its frequency is much higher than the maximum vibrational frequency of the perfect (host) lattice. (c) The vibrational spectrum exhibits predominantly "one-mode" behavior¹¹ over the entire range of concentrations. It is interesting to note, however, that the modes at 139 and 153 cm^{-1} in phase III show typical "two-mode" behavior. A similar situation has also been reported¹² for the solid solution: $\text{Ba}_2(\text{K}_x\text{Na}_{1-x})\text{Nb}_5\text{O}_{15}$ with tungsten-bronze structure.

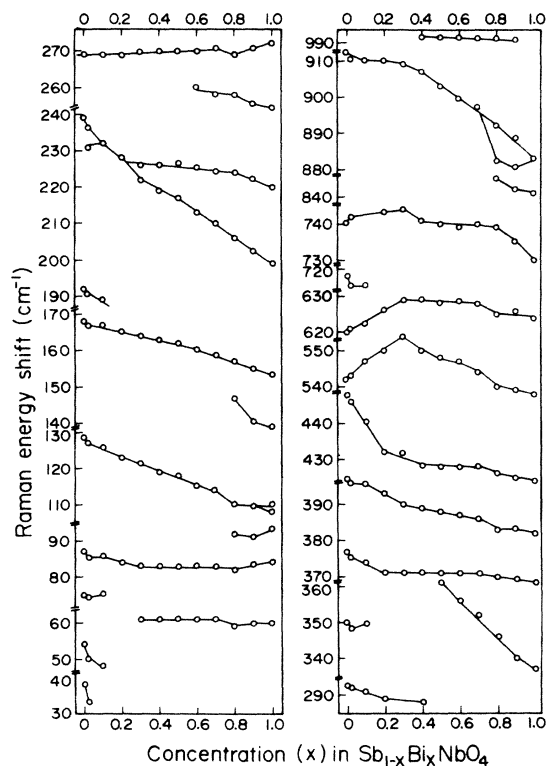


FIG. 3. The variation of the Raman frequencies with concentration (x) in $(\text{Sb}_{1-x}\text{Bi}_x)\text{NbO}_4$ for $0 \leq x \leq 1.0$.

V. LATTICE VIBRATIONS AND SOFT MODES

Displacive ferroelectrics normally have at least one low-energy TO mode which softens as the ferroelectric T_C is approached. Similarly, one or more vibrational modes in a solid solution may soften when a structural phase transition (SPT) is approached by varying x at constant T . In SbNbO_4 , the Raman mode at 37 cm^{-1} is likely to be the soft TO mode. At $x = 0.02$ this mode is damped and barely visible, and it softens rapidly for higher x . Hence, this mode appears to be responsible for the concentration-dependent SPT near $x = 0.2$. Another low-lying mode (around 50 cm^{-1}), which occurs strongly in the ir but weakly in the Raman, appears to be coupled to the soft mode for it decreases in frequency and vanishes at $x = 0.2$. In fact, a number of low-lying modes (below $80\text{--}100$

cm^{-1}) were found in all the four ABO_4 type compounds investigated. Such modes may be expected to play significant roles in the multiple transitions exhibited by these systems.

Frequencies falling below $180\text{--}200 \text{ cm}^{-1}$ are usually ascribed to translatory motions involving cations. For a majority of these modes the frequency decreases monotonically from the Sb (lighter mass) to the Bi end. Such a behavior would obviously follow if we naively assume the force constants to be independent of x . An approximate idea of the magnitudes of the force constants actually involved may be obtained from the Born—von Kármán description of a one-dimensional lattice, which is reasonably accurate in spite of its crude nature. The zone-center TO frequency is given by $\omega_{\text{TO}}^2 = 2f/\mu$, where f is the central force constant and μ , the reduced mass of the system. When we consider the A sublattice moving as a whole against the BO_6 octahedra, $\mu^{-1} = m_A^{-1} + m_{\text{BO}_6}^{-1}$. Considering the Raman line at 128.5 cm^{-1} in SbNbO_4 and at 109 cm^{-1} in BiNbO_4 , we obtain the following values for the corresponding force constants:

$$f(\text{SbNbO}_4) = 0.360 \text{ m dyn}/\text{\AA} ,$$

$$f(\text{BiNbO}_4) = 0.347 \text{ m dyn}/\text{\AA} .$$

Hence the shift in frequency with x is predominantly a mass effect. Two of the lattice modes (near 60 and 84 cm^{-1}), however, appear to be almost independent of x . These may be reasonably expected to arise from motions of the Nb^{5+} ions against each other.

Raman spectra of the two end members were also recorded near 150 K in quartz tubes (Harney-Miller cell) cooled by passing cold and dry nitrogen gas. No significant changes were observed in the frequencies of either lattice or internal modes, showing the absence of any SPT between RT and 150 K . Finally, we wish to make a comment regarding the Raman linewidths. It is apparent from Fig. 1 that the Raman bands above 200 cm^{-1} are considerably broader than those below. Such a situation is not uncommon in polycrystalline samples. The rather large linewidths may be assigned to the slightly asymmetric nature of the NbO_6 octahedra. The Nb—O bond lengths in SbNbO_4 , for example,¹ vary between 1.874 and 2.058 \AA . The lowering of symmetry would partially lift the degeneracies in the vibrational modes of the ideal octahedra and result in the observed line broadening.

¹V. I. Popolitov, A. N. Lobachev, and V. F. Peskin, *Ferroelectrics* **40**, 9 (1982).

²A. P. Leonov, S. Yu. Stefanovich, L. L. Kukueva, and Yu. N. Venetsev, *Kristallografiya* **29**, 1027 (1984) [*Sov. Phys. Crystallogr.* **29**, 603 (1984)].

³Pushan Ayyub, V. R. Palkar, M. S. Multani, and R. Vijayaraghavan (unpublished).

⁴Yu. N. Venetsev, L. A. Ivanova, and S. A. Oconenko, *Ferroelectrics* **13**, 515 (1976).

⁵D. L. Rousseau, R. P. Bauman, and S. P. S. Porto, *J. Raman Spectrosc.* **10**, 253 (1981).

⁶W. Jeitschko and A. W. Sleight, *Acta Crystallogr. Sect. B* **30**,

2088 (1974).

⁷A. A. McConnell, J. S. Anderson, and C. N. R. Rao, *Spectrochim. Acta Part A* **32**, 1067 (1976).

⁸See, e.g., L. H. Jones, *Inorganic Vibrational Spectroscopy* (Marcel Dekker, New York, 1971), Vol. 1.

⁹E. B. Wilson, J. C. Decius, and P. C. Cross, *Molecular Vibrations* (McGraw-Hill, New York, 1955).

¹⁰S. D. Ross, *J. Phys. C* **3**, 1785 (1970).

¹¹I. F. Chang and S. S. Mitra, *Adv. Phys.* **20**, 359 (1971).

¹²A. Boudou, J. Sapriel, B. Joukoff, R. Mellet, G. Le Roux, and D. Morin, *Phys. Rev. B* **22**, 1170 (1980).